Computers and Chemical Engineering 144 (2021) 107156

Contents lists available at ScienceDirect

Computers and Chemical Engineering

journal homepage: www.elsevier.com/locate/compchemeng

An online operating performance evaluation approach using probabilistic fuzzy theory for chemical processes with uncertainties

Yalin Wang, Ling Li*, Kai Wang*

School of Automation, Central South University, Changsha, Hunan 410083, China

ARTICLE INFO

Article history:
Received 16 March 2020
Revised 28 September 2020
Accepted 1 November 2020
Available online 2 November 2020

Keywords:
Operating performance evaluation (OPE)
Stochastic uncertainty
Fuzzy uncertainty
Probabilistic fuzzy inference
Variable selection

ABSTRACT

Operating performance evaluation (OPE) has been playing an essential role to ensure the effective operations of chemical processes. However, most of previous research focused on the deterministic evaluation strategies, without consideration of uncertainties in the evaluation indicators of OPE. Based on probabilistic fuzzy theory, an online OPE scheme is proposed by considering the uncertainties in chemical processes. In the modeling step, on the basis of just-in-time learning and probabilistic principal component regression, a prediction model is proposed and applied to estimate the probability distribution of the evaluation indicators in real time; and a weighted cosine Mahalanobis-Taguchi system for variable selection is developed to improve the prediction accuracy of the evaluation indicators. In the evaluation step, a probabilistic fuzzy inference method is proposed to improve the accuracy of evaluation results by considering the uncertainty of evaluation indicators. The effectiveness of the proposed approach is finally tested on an industrial hydrocracking process.

1. Introduction

Operating optimization of chemical processes has received much attention with the development of intelligent manufacturing and the goal of green and highly efficient industrial production (Wang et al., 2019a). However, the process operating performance may deviate from the optimal condition due to process parameter drift and environment disturbance such as feedstock component fluctuation, equipment scaling, and lack of instrument maintenance, etc. Hence, it is of great significance to evaluate the process operating performance timely and accurately.

Operating performance evaluation (OPE) has attracted its attention in both academia community and industry community. Especially, not only in chemical engineering, the relevant studies have also been carried out in management science. Molinos Senante et al. developed a comprehensive indicator which embracing economic, environmental and social issues when evaluating the sustainability of wastewater treatment systems (Molinos-Senante et al., 2014). K. S. Chen et al. developed a performance index of manufacturing time and applied it to the evaluation of production performance (Chen et al., 2006). B. Shiva Kumar and K. Sudhakar evaluated the performance of 10MW grid connected solar photovoltaic power plant in India, in which various types of power losses and performance ratio are calculated (Kumar and Sudhakar, 2015). However, the calculation of evaluation indicators in these approaches needs to collect enough data over a long period of time, which will lead to a serious evaluation lag (Wang et al., 2020). In other words, even though offline evaluation can be achieved, it will possibly suffer an unacceptable evaluation lag so that just a seriously delayed decision would be made. Thus, online evaluation is urgently needed for practical chemical processes.

To achieve online evaluation, soft sensors (Chen et al., 2019; Chen and Jiang, 2019; Hiromasa and Kimito, 2013) have been constructed to realize real-time estimation for the evaluation indicators. Liu et al., Zou and Chang et al. proposed a series of OPE methods for multimode processes based on multiple data-driven evaluation indicator prediction methods (Liu et al., 2014b; Liu et al., 2016, 2018; Chang et al., 2018; Zou et al., 2018). Li et al. recently proposed a two-layer fuzzy synthetic strategy for OPE of an industrial hydrocracking process (Li et al., 2019). This method was based on a fuzzy evaluation method, where partial least squares (PLS) was applied for predicting indicators. However, these existing methods ignore the uncertain effects of process data and evaluation indicators. In fact, the process data are collected under the uncertainties caused by process noise and measurement noise. It will make a lot of sense that the model accuracy can be explicitly represented given a significance level if the predictive results of the evaluation indicators are described by probability distributions.

* Corresponding authors.
E-mail addresses: lilings@csu.edu.cn (L. Li), kaiwang@csu.edu.cn (K. Wang).

https://doi.org/10.1016/j.compchemeng.2020.107156
0098-1354/

Moreover, as the accurate prediction of evaluation indicators seriously affects the accuracy of OPE, how to quickly and effectively select a set of process variables that can most exactly describe or explain the process is particularly important. Researchers have proposed several approaches for variable selection. Jiang et al. proposed a relative decision entropy-based feature selection method, which was an extension of Shannon's information entropy in rough sets (Jiang et al., 2015). Sun et al. used information theoretic criteria to analysis feature relevance, interdependence and redundancy (Sun et al., 2013). Liu et al. developed a feature selection method with ultrahigh-dimensional covariates based on conditional correlation coefficients (Liu et al., 2014a). However, working conditions are not considered and captured in these methods. As a matter of fact, working conditions are crucial in variable selection. Because the switch of working conditions will result in the changes in the degree of influence of process variables on process indicators. Therefore, Wu et al. proposed an unsupervised reduction method for characters selection of flotation froth image, in which characters that strongly related to the working conditions of the flotation process were first selected based on a sensitivity index (Wu et al., 2014). Then, rough set attribute importance method was further used to deal with the correlation problem existing in the selected sensitive image characters. However, this approach neglects the correlations between the indicators and the process variables, which may cause the selected variables to be suboptimal.

To address the above problems of online OPE with uncertainties and variable selection in the construction of evaluation indicator prediction model, an online probabilistic fuzzy evaluation approach is proposed for operating performance of chemical processes with uncertainties. The approach can be decomposed into modeling step and evaluation step. In the modeling step, a weighted cosine Mahalanobis-Taguchi system (WCMTS) for variable selection is firstly developed to improve the prediction accuracy of the evaluation indicators. Sensitive variables (SV) and key sensitive variables (KSV) are first defined in this variable selection method, in which SV represents the process variables that are closely to the evaluation indicators, while KSV refers to the redundancy-removed SV. Then, a sensitivity index (SI) is developed to select SV preliminarily, and KSV can be precisely selected by WCMTS. After that, a prediction model based on just-in-time-learning and probabilistic principal component regression (JITL-PPCR) is applied to estimate the probability distribution of the evaluation indicators in real-time. As mentioned above, a weighted cosine Mahalanobis-Taguchi system based just-in-time-learning and probabilistic principal component regression (WCMTS-JITL-PPCR) method is developed for estimating evaluation indicators. In the evaluation step, a probabilistic fuzzy inference method is proposed, wherein three types of traditional fuzzy membership functions are extended to probabilistic fuzzy memberships. By considering the uncertainty of evaluation indicators, the probabilistic fuzzy inference method improves the accuracy of evaluation results.

Compared with the existing online OPE approaches, novelty and contributions of the proposed method can be summarized as follows.

(1) An effective online OPE method based on probabilistic fuzzy inference is proposed, which can obtain better evaluation performance under uncertainties.
(2) A variable selection method is developed for reducing the model complexity and improving the prediction accuracy for the evaluation indicators.
(3) Based on the variable selection, a JITL-PPCR strategy is proposed for describing the probability distribution of the predicted evaluation indicators, which can improve the prediction performance in nonlinear time-varying processes with noise.

The remainder of this paper is structured as follows. In Section 2, motivation and framework for PFES are discussed. Section 3 describes the WCMTS-JITL-PPCR based modeling and the probabilistic fuzzy evaluation strategy with uncertainties in detail. Then, the effectiveness and performance of the proposed methods are validated on an industrial hydrocracking process in Section 4. At last, conclusions are given in Section 5.

2. Motivation and framework for PFES

In general, process operating performance changes slowly and is difficult to quantify. To deal with this fuzzy uncertainty problem, fuzzy synthetic evaluation (Kumar et al., 2007; Pai et al., 2009) has been constructed to give an exact evaluation result. Suppose that the set of objects to be evaluated is denoted as$U = \{u_1, u_2, \ldots, u_n\}$, and the set of evaluation levels is $V = \{v_1, v_2, \ldots, v_m\}$. Fuzz each object according to the level indicator in the evaluation level set, an evaluation matrix can be obtained

$$\mathbf{B} = \begin{bmatrix} b_{11} & b_{12} & \cdots & b_{1m} \\ b_{21} & b_{22} & \cdots & b_{2m} \\ \vdots & \vdots & \vdots & \vdots \\ b_{n1} & b_{n2} & \cdots & b_{nm} \end{bmatrix}, \tag{1}$$

where $b_{ij}(i = 1, \ldots, n; j = 1, \ldots, m)$ represents the membership value of u_i with respect to v_j. After that, construct a weight matrix as$\mathbf{A} = [\ a_1 \quad a_2 \quad \cdots \quad a_n\ ](\sum_{i=1}^{n} a_i = 1)$, then the evaluation result can be obtained by fuzzy synthetic as

$$\mathbf{L} = \mathbf{A} \circ \mathbf{B} = \begin{bmatrix} l_1 & l_2 & \cdots & l_m \end{bmatrix}, \tag{2}$$

where$\circ$ represents matrix multiplication, $l_i(i = 1, \cdots, m)$ is the membership of the evaluation level. According to the principle of maximum membership, the final evaluation result is the evaluation level with the highest membership. Fig. 1 shows a traditional fuzzy synthetic evaluation system, which includes fuzzification, weight construction and fuzzy synthetic. The crisp inputs of the system are deterministic, which are obtained from soft sensor models. As mentioned above, the indicators are actually inherently random variables. From the perspective of statistical viewpoints, it is more appropriate that data analysis and decisions be made in a probabilistic manner.

In this paper, a probabilistic fuzzy synthetic evaluation approach of process operating performance with uncertainties is proposed, Fig. 2 shows the probabilistic fuzzy evaluation system. As the inputs of the system are probability distribution functions centered on the predictive indicators, the fuzzification in the traditional fuzzy synthetic evaluation should be extended to probabilistic fuzzification where the traditional fuzzy memberships are also extended to the corresponding probabilistic counterparts, i.e., probabilistic fuzzy memberships. Thus, the traditional two-dimensional fuzzy set should be extended to a three-dimensional probabilistic fuzzy set, in which each dimension represents the codes of input variable x, fuzzy membership value$\mu(x)$, and the probability of input variable x, respectively. Obviously, $\mu \in [0, 1]$ and $p(\mu) \geq 0, \int_0^1 p(\mu)d\mu = 1$.

3. WCMTS-JITL-PPCR based modeling and PFES

Probabilistic fuzzy evaluation with uncertainties consists of model construction and performance evaluation. A WCMTS-JITL-PPCR method is firstly developed for evaluation indicators estimation, which can be further decomposed into two parts: variable selection and process modeling. Then, the probabilistic fuzzy strategy is proposed to achieve the operating performance evaluation. An overview of the proposed approach is given in Fig. 3, and the details are described in the following sections.

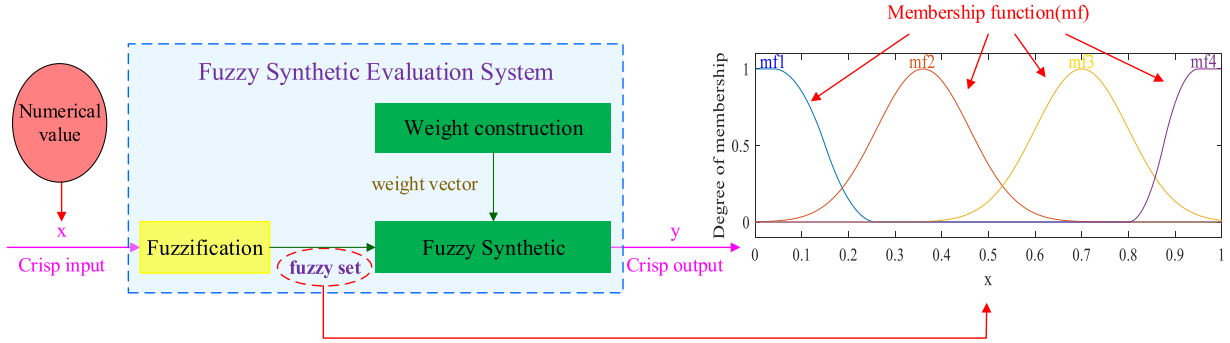

Fig. 1. Configuration of the traditional fuzzy synthetic evaluation system.

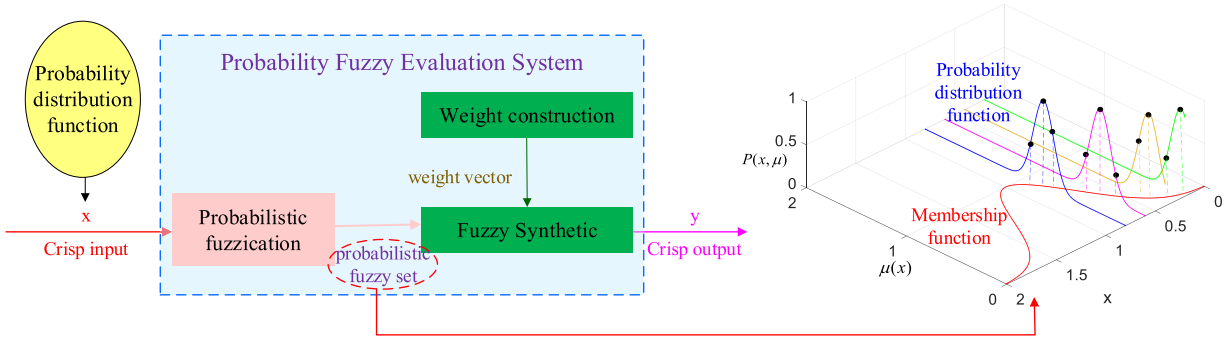

Fig. 2. Configuration of the probabilistic fuzzy evaluation system.

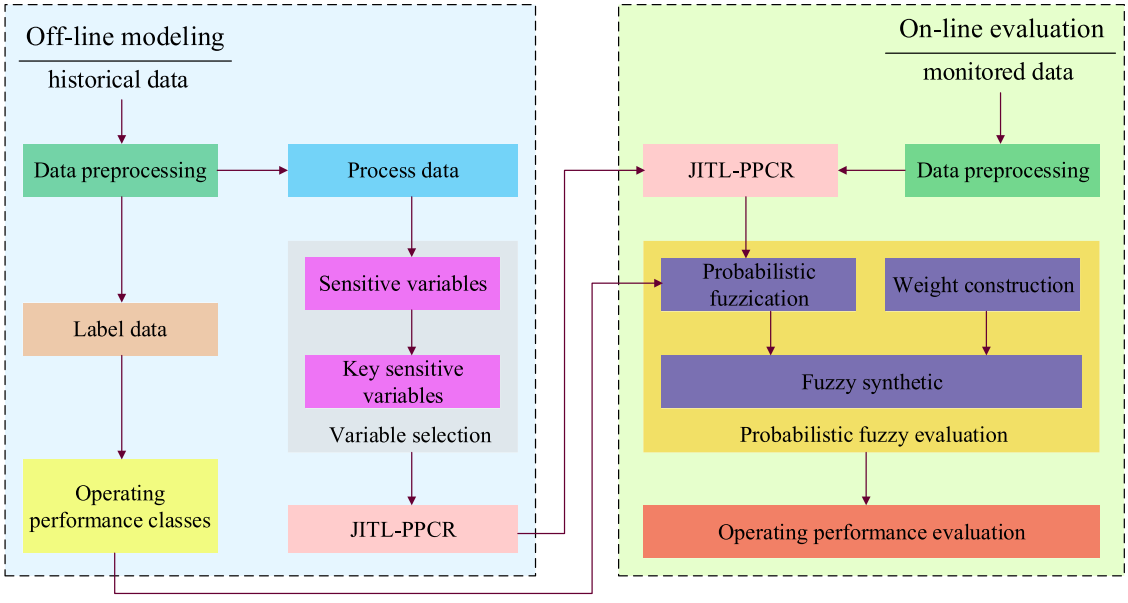

Fig. 3. An overview of the proposed framework and methods for off-line training and on-line assessment.

3.1. Variable selection based on WCMTS

As mentioned, it is very important to select an optimal explanatory variable subset from the measured variables for a predictive model. First, assume that the set of all available process data is represented as P, then two crucial concepts can be derived from the characteristics of the variable selection process.

Concept 1: Sensitive variables (SV) set, denoted as P^S, includes the process variables which are closely related to the evaluation indicators given by a specific working condition. However, due to the redundancy caused by correlations between the sensitive variables, the selected variables may be suboptimal. Therefore, it is necessary to further select key sensitive variables to eliminate redundancy.

Concept 2: Key sensitive variables (KSV) set consists of the redundancy-removed sensitive variables and is represented by P^K.

Obviously, the following relationship exists between SV and KSV

$$P^K \subseteq P^S \subseteq P \tag{3}$$

3.1.1. Sensitive variables selection

Without loss of generality, data preprocessing should be carried out before SV selection, including outlier elimination and data

normalization. Suppose the process variables can be represented as$\mathbf{X} \in \mathbf{R}^{n\times m}$, where n and m are the number of sample data and the dimension of process variables, respectively. The data normalization can be represented as follows

$$z_{ij} = (x_{ij} - \mu_j)/s_j, \tag{4}$$

wherex_{ij} represents the i^{th} sample of the j^{th} variable, μ_j represents the mean value of the j^{th} variable, s_j represents the standard deviation of the j^{th} variable.

Concept 3: Consider a certain period of time with several working conditions, sensitivity index (SI) is the product of the dispersion degree of process variables and the correlation that between process variables and evaluation indicators, which can be regarded as

$$\eta_{jk} = \begin{cases} r_{jk} * \frac{s_j}{|\mu_j|} & \mu_j \neq 0 \\ r_{jk} * \sigma_j & \mu_j = 0 \end{cases}, \tag{5}$$

where r_{jk} represents the partial correlation coefficient of the j^{th} variable and the k^{th} evaluation indicator, μ_j represents the mean value of the j^{th} variable, s_j represents the standard deviation of the j^{th} variable, and σ_j is the variance of the j^{th} variable. The partial correlation coefficient can exclude the influence of other variables, and calculate the correlation coefficient between the current variable and the target variable, that is, the net correlation, which can achieve more accurate variable selection. The calculation process of the partial correlation coefficient is as follows.

Firstly, calculate the correlation coefficient matrix by using Pearson correlation analysis method (Nishiguchi and Takai, 2010) as follows

$$\mathbf{M}_{cc} = \begin{bmatrix} \omega_{11} & \omega_{12} & \cdots & \omega_{1m} \\ \omega_{21} & \omega_{22} & \cdots & \omega_{2m} \\ \vdots & \vdots & \cdots & \vdots \\ \omega_{m1} & \omega_{m2} & \cdots & \omega_{mm} \end{bmatrix}, \tag{6}$$

where$\omega_{jk} = L_{jk}/\sqrt{L_{jj}L_{kk}}, j = 1, \ldots, m; k = 1, \ldots, m;\quad L_{jk} = \sum_{i=1}^{n} z_{ij}z_{ik} - \frac{1}{n}\sum_{i=1}^{n} z_{ij}\sum_{i=1}^{n} z_{ik}$.

The partial correlation coefficient r_{jk} of the process variable z_j and evaluation indicator v_k can be regarded as

$$r_{jk} = \frac{-c_{jk}}{\sqrt{c_{jj}c_{kk}}}, j = 1, \ldots, m, k = 1, \ldots, m, \tag{7}$$

$$\mathbf{M}_{cc}^{-1} = \begin{bmatrix} c_{11} & c_{12} & \cdots & c_{1m} \\ c_{21} & c_{22} & \cdots & c_{2m} \\ \vdots & \vdots & \cdots & \vdots \\ c_{m1} & c_{m2} & \cdots & c_{mm} \end{bmatrix}, \tag{8}$$

where c_{jk} is the element of the inverse matrix $\mathbf{M}_{cc}^{-1}$ of $\mathbf{M}_{cc}$.

The larger the SI, the greater the influence of the process variable on the evaluation indicator and the more sensitive it is to the changes in working conditions.

3.1.2. Key sensitive variables selection

To eliminate the redundancy, a WCMTS is developed in this section. Mahalanobis-Taguchi system (MTS) (Chang et al., 2019; Mahalakshmi and Ganesan, 2009; Soylemezoglu et al., 2011) is an effective pattern recognition technology and dimension reduction tool developed by Dr. Genichi Taguchi based on mahalanobis distance (MD) and Taguchi method. The method has been widely used in product testing, disease diagnosis, credit audit and so on. Traditional MTS includes constructing mahalanobis space (MS) based on MD where MD is utilized to identify data anomalies, verify the MS, and optimize the MS by using orthogonal arrays (OAs) and signal-to-noise ratios (S/N ratios). However, it is demonstrated that selecting similar samples based on distance information alone does not always function well, because angle information is also important (Yuan et al., 2018). Therefore, it is necessary to construct a new measurement scale to improve the classification accuracy and expand its application scope.

Cosine similarity (CS) is a commonly used similarity measurement, which is defined as the inner product of the two vectors divided by the product of their lengths. Combining CS and MD, a new metric of cosine mahalanobis distance (CMD) is proposed, which can not only retain the advantages of MD, but also make up for the shortcomings that the abnormalities cannot be identified from the perspective of direction in MTS.

The procedure of WCMTS is detailed as follows.

Step 1: Select and normalize n normal observations where each observation has q process variables

$$\widetilde{\mathbf{O}} = \begin{bmatrix} \widetilde{o}_{11} & \widetilde{o}_{12} & \cdots & \widetilde{o}_{1q} \\ \widetilde{o}_{21} & \widetilde{o}_{22} & \cdots & \widetilde{o}_{2q} \\ \vdots & \vdots & \cdots & \vdots \\ \widetilde{o}_{n1} & \widetilde{o}_{n2} & \cdots & \widetilde{o}_{nq} \end{bmatrix}, \tag{9}$$

where $\widetilde{o}_{ij}$ is the normalized data of the j^{th} sensitive variable of the i^{th} sample.

Step 2: Calculate the MDs of normal observations. The MD_i corresponding to the i^{th} observation can be represented as

$$MD_i = \frac{1}{q}\widetilde{\mathrm{O}}_i\mathbf{S}^{-1}\widetilde{\mathbf{O}}_i^T, i = 1, 2, \ldots n, \tag{10}$$

where $\mathbf{S} = \frac{1}{n-1}\sum_{i=1}^{n}\widetilde{\mathbf{O}}_i^T\widetilde{\mathbf{O}}_i$ is the correlation matrix.

Step 3: Calculate the CSs of normal observations. In order to effectively combine the evaluation criteria based on CS and MD, the paper deforms the traditional CS formula as follows

$$CS_i = \frac{1}{\cos i + 2} = \frac{1}{\frac{\widetilde{\mathbf{o}}_i\cdot\overline{\mathbf{o}}}{\|\widetilde{\mathbf{o}}_i\|\cdot\|\overline{\mathbf{o}}\|} + 2}, \tag{11}$$

where $\widetilde{\mathbf{o}}_i (i = 1, 2, \ldots, n)$ represents the i^{th} sample, and $\overline{\mathbf{o}}$ is the mean vector of the normal observations.

Step 4: Calculate the CMDs of normal observations. The *CMD* of the i^{th} observation can be represented as

$$CMD_i = \alpha MD_i + \beta CS_i, \tag{12}$$

where α and β are the weights determined by the dispersions of MDs and CSs of the normal samples, respectively. The weight calculation process is shown as follows

$$\alpha = \frac{\psi_1}{\psi_1 + \psi_2}\beta = \frac{\psi_2}{\psi_1 + \psi_2}, \tag{13}$$

$$\psi_1 = \frac{s_{MDi}}{\mu_{MDi}}, \tag{14}$$

$$\psi_2 = \frac{s_{CSi}}{\mu_{CSi}}, \tag{15}$$

where ψ_1 and ψ_2 are the dispersions of MDs and CSs, respectively; s_{MDi} and s_{CSi} are the standard deviations of MDs and CSs, respectively; μ_{MDi} and μ_{CSi} are the mean values of MDs and CSs, respectively. The benchmark space consisting of all CMDs of the normal observations is called weighted cosine mahalanobis space (WCMS).

Step 5: Verify the effectiveness of the WCMS. By using the same mean and standard deviation of the normal samples, the abnormalities can be normalized. Then, calculate the CMDs of the abnormalities based on the constructed WCMS. If the constructed WCMS is valid, the CMDs of the abnormalities should be higher.

Step 6: Optimize the WCMS by using OAs and S/N ratios. First, a two-level OAs should be designed to identify the useful process variables, in which each row corresponds to a benchmark space. Level-1 means including the variable, while level-2 means excluding the variable. Then, calculate the CMDs of the abnormalities in each benchmark space. After that, calculate the S/N ratios (the larger-the-better type S/N ratios is frequently suggested) according to Eq. (16).

$$SNR = -10\left[(1/m)\sum_{p=1}^{m}(1/CMD_p)\right], \tag{16}$$

where CMD_p is the CMD of the p^{th} abnormal sample, m is the number of abnormal samples. For each variable, calculate its effective gain of S/N ratios by Eq. (17)

$$\Delta SN = \overline{SN}_{level-1} - \overline{SN}_{level-2}, \tag{17}$$

where $\overline{SN}_{level-1}$ represents the average S/N ratios at level-1, $\overline{SN}_{level-2}$ represents the average S/N ratios at level-2. The variables with positive ΔSN are worth keeping, while the rest are discarded. To eliminate the redundant variables to a greater extent, a certain threshold can be set for ΔSN.

3.2. Evaluation indicators estimation based on JITL-PPCR

To calculate the evaluation indicators in real time, various kinds of soft sensor methods can be utilized, such as neural network (Wang et al., 2019b; Sun et al., 2020), support vector machine (Qi et al., 2011; Yang et al., 2011), partial least squares (Chen et al., 2019b; Fuat et al., 2003), principal component regression (Yuan et al., 2014; Zheng and Song, 2017) and so on. However, the inevitable process noise is not considered in these models, which may lead to the failure or performance degradation in modeling. To improve the prediction performance in nonlinear time-varying processes with noise, JITL-PPCR is applied in the paper.

Following the principles of probabilistic principal component regression (PPCR) (Chen et al., 2019a; Sedghi et al., 2017; Zhu et al., 2015) and just-in-time-learning (JITL) (Ge and Song, 2010; Zhou et al., 2020), JITL-PPCR can be built as

$$\mathbf{x} = \mathbf{Pt} + \mathbf{e} \tag{18}$$

$$\mathbf{y} = \mathbf{Ct} + \mathbf{f} \tag{19}$$

where $\mathbf{P} \in R^{m\times q}$ and $\mathbf{C} \in R^{r\times q}$ are the corresponding loading matrix and regression matrix; $\mathbf{t} \in R^{q\times 1}$ is the principal component vector, which is assumed to be Gaussian $p(\mathbf{t}) = N(0, \mathbf{I})$; where $\mathbf{I}$ is an identity matrix; $\mathbf{e} \in R^{m\times 1}$ and $\mathbf{f} \in R^{r\times 1}$ are process noises of the measurement and predicted variables, respectively, which are also assumed to be Gaussian $p(\mathbf{e}) = N(0, \sigma_{\mathbf{x}}^2\mathbf{I})$ and $p(\mathbf{f}) = N(0, \sigma_{\mathbf{y}}^2\mathbf{I})$, where $\sigma_{\mathbf{x}}^2$ and $\sigma_{\mathbf{y}}^2$ are corresponding noise variances. The flowchart of JITL-PPCR modeling procedure is displayed in Fig. 4.

The difference between PPCR and JITL-PPCR is that PPCR extract latent variables from original input data while JITL-PPCR extracts latent variables from local input data. In the JITL-PPCR model, the local input data are from the historical dataset around a query data sample. This leads to a fact that PPCR only extracts linear features while JITL-PPCR can extract nonlinear features. Therefore, the evaluation indicator can be described as $p(y) = N(\hat{y}, \sigma_y^2\mathbf{I})$.

3.3. OPE based on PFES

Due to the stochastic uncertainty of predictive indicators and the fuzzy uncertainty of operating performance evaluation, a probabilistic fuzzy evaluation strategy is proposed in this section. The proposed probabilistic fuzzy evaluation consists of probabilistic fuzzification of evaluation indicators, weight vector construction, and evaluation matrix calculation. As weight vector construction and evaluation matrix calculation are the same as traditional fuzzy synthetic evaluation, only probabilistic fuzzification is introduced in detail.

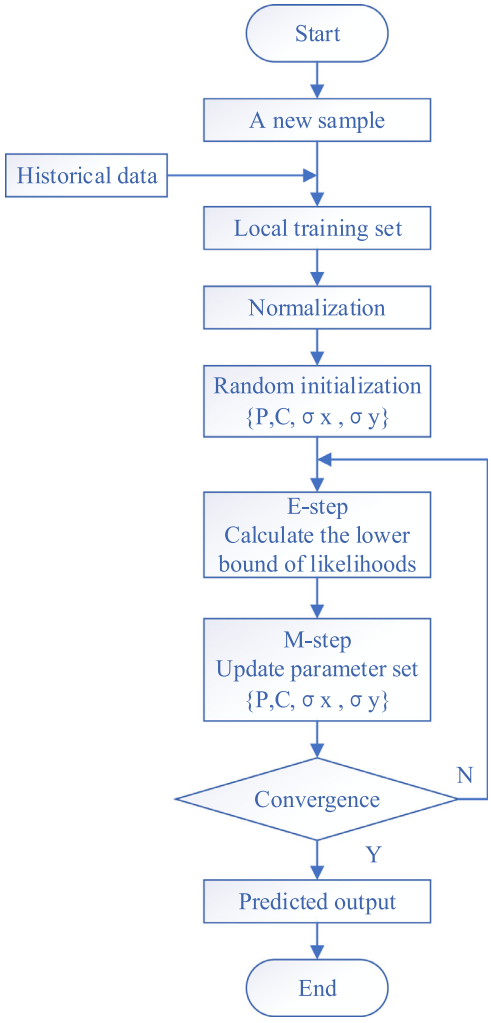

Fig. 4. The flowchart of JITL-PPCR modeling procedure.

3.3.1. Traditional fuzzification

Once evaluation indicators are prepared, these quantitative variables can be transformed into linguistic variables through fuzzification. Typical membership function types (Takagi and Sugeno, 1993; Zhang et al., 2016) include trapezoidal, triangle, S-shaped, Z-shaped, bell-shaped, Gaussian distribution, etc. Triangle and trapezoidal membership functions are the most commonly used fuzzy membership functions. However, the curves of these two membership functions are too sharp and cannot fit the actual production process well. Therefore, to better fit the production process, three more smooth membership functions are chosen, which are S-shaped, Z-shaped, and Gaussian-shaped membership functions. The S-shaped functions are represented as Eq. (20).

$$\varphi^j(x) = \begin{cases} 1, & x \le \alpha^j \\ 1 - 2\left(\frac{x-\alpha^j}{\beta^j-\alpha^j}\right)^2, & \alpha^j \le x \le \frac{\alpha^j+\beta^j}{2} \\ 2\left(\frac{x-\beta^j}{\beta^j-\alpha^j}\right)^2, & \frac{\alpha^j+\beta^j}{2} \le x \le \beta^j \\ 0, & x \ge \beta^j \end{cases}, \tag{20}$$

where α^j and β^j are the parameters that determine the slope of function curve. The Z-shaped functions are represented as Eq. (21).

$$\psi^j(x)=\begin{cases}0, & x\le c^j\\ 2\left(\frac{x-c^j}{d^j-c^j}\right)^2, & c^j\le x\le \frac{c^j+d^j}{2}\\ 1-2\left(\frac{x-d^j}{d^j-c^j}\right)^2, & \frac{c^j+d^j}{2}\le x\le d^j\\ 1, & x\ge d^j\end{cases}, \tag{21}$$

where c^j and d^j are the parameters that determine the slope of function curve. The Gaussian-shaped functions are represented as Eq. (22).

$$\mu_i^j(x)=e^{-\frac{(x-\xi_i^j)^2}{2(\sigma_i^j)^2}}, \tag{22}$$

where ξ_i^j and σ_i^j are the center and width of the function curve, respectively.

3.3.2. Probabilistic fuzzification

As the evaluation indicators are no longer deterministic values but probability distribution functions, the traditional fuzzification is no longer applicable, which should be extended to probabilistic fuzzification as follows.

$$\vartheta^j(x)=\int \upsilon^j(x)p(x)dx, \tag{23}$$

where $\vartheta^j(x)$ represents the probabilistic fuzzy membership functions, $\upsilon^j(x)$ represents the fuzzy membership functions, and $p(x)$ represents the probability distribution functions of the evaluation indicators. Then the S-shaped probabilistic fuzzy membership functions can be extended as Eq. (24).

$$\begin{aligned}\varphi^j(x)' =& \sqrt{\frac{\pi}{2}}\sigma_x+\frac{2\sqrt{2}\sigma_x^3}{\left(\beta^j-\alpha^j\right)}k_3\exp\left(-k_1^2\right)\\ &-\left(\frac{4\sqrt{2}\sigma_x^3}{\left(\beta^j-\alpha^j\right)^2}k_1+\frac{4\sqrt{2}\sigma_x^3}{\left(\beta^j-\alpha^j\right)^2}k_3\right)\exp\left(-k_2^2\right)\\ &+\frac{6\sqrt{2}\sigma_x^3}{\left(\beta^j-\alpha^j\right)^2}k_3\exp\left(-k_3^2\right)+\frac{2\sqrt{2}\sigma_x^3\left(1+2k_1^2\right)}{\left(\beta^j-\alpha^j\right)^2}erf(k_1)\\ &+\left(\sqrt{2}\sigma_x-\frac{4\sqrt{2}\sigma_x^3}{\left(\beta^j-\alpha^j\right)^2}-\frac{4\sqrt{2}\sigma_x^3}{\left(\beta^j-\alpha^j\right)^2}k_1^2\right.\\ &\left.-\frac{4\sqrt{2}\sigma_x^3}{\left(\beta^j-\alpha^j\right)^2}k_3^2\right)erf(k_2)\\ &+\frac{6\sqrt{2}\sigma_x^3}{\left(\beta^j-\alpha^j\right)^2}erf(k_3)\end{aligned}, \tag{24}$$

where $k_1=\frac{\alpha^j-\widehat{x}}{\sqrt{2}\sigma_x}$, $k_2=\frac{(\alpha^j+\beta^j)/2-\widehat{x}}{\sqrt{2}\sigma_x}$, $k_3=\frac{\beta^j-\widehat{x}}{\sqrt{2}\sigma_x}$; α^j and β^j are the parameters that determine the slope of function curve, respectively; $\widehat{x}$ is the predictive value of the evaluation indicator, σ_x is the variance of the predictive value; and *erf(x)* is an introduced non-elementary function, which is the error function of x and can be represented as $erf(x)=\int_0^x e^{-t^2}dt$. The Z-shaped probabilistic fuzzy membership functions are represented as Eq. (25).

$$\begin{aligned}\psi^j(x)' =& \sqrt{\frac{\pi}{2}}\sigma_x-\frac{2\sqrt{2}\sigma_x^3}{\left(d^j-c^j\right)^2}t_1\exp\left(-t_1^2\right)\\ &+\left(\frac{4\sqrt{2}\sigma_x^3}{\left(d^j-c^j\right)^2}(t_1-t_2)\right)\exp\left(-t_2^2\right)\\ &+\frac{2\sqrt{2}\sigma_x^3}{\left(d^j-c^j\right)^2}t_3\exp\left(-t_3^2\right)+\frac{4\sqrt{2}\sigma_x^3}{\left(d^j-c^j\right)^2}\left(\frac{1}{2}-t_1^2\right)erf(t_1)\\ &+\left(\frac{4\sqrt{2}\sigma_x^3}{\left(d^j-c^j\right)^2}\left(t_1^2-t_3^2\right)-\sqrt{2}\sigma_x\right)erf(t_2)\\ &-\left(\frac{2\sqrt{2}\sigma_x^3}{\left(d^j-c^j\right)^2}\left(1-2t_3^2\right)\right)erf(t_3)\end{aligned}, \tag{25}$$

where $t_1=\frac{c^j-\widehat{x}}{\sqrt{2}\sigma_x}$, $t_2=\frac{(c^j+d^j)/2-\widehat{x}}{\sqrt{2}\sigma_x}$, $t_3=\frac{d^j-\widehat{x}}{\sqrt{2}\sigma_x}$; c^j and d^j are the parameters that determine the slope of function curve, respectively; $\widehat{x}$ is the predictive value of the evaluation indicator, σ_x is the variance of the predictive value; and *erf(x)* is the introduced non-elementary function. The Gaussian-shaped probabilistic memberships can be represented as Eq. (26).

$$\begin{aligned}\mu_i^j(x)' =& \sqrt{\frac{\pi}{\sigma_x^2+\left(\sigma_i^j\right)^2}}\left(\left(\sigma_x^2\xi_i^j+\left(\sigma_i^j\right)^2\widehat{x}\right)^2\right)\\ &\exp\left(-\sigma_x^2\left(\xi_i^j\right)^2-\left(\sigma_i^j\right)^2\widehat{x}^2+\frac{\left(\sigma_x^2\xi_i^j+\left(\sigma_i^j\right)^2\widehat{x}\right)^2}{\sigma_x^2+\left(\sigma_i^j\right)^2}\right)\end{aligned}, \tag{26}$$

where ξ_i^j and σ_i^j are the center and width of the function curve, respectively; $\widehat{x}$ is the predictive value of the evaluation indicator, σ_x is the variance of the predictive values. The detailed derivation of Eqs. (24)–(26) can be found in Appendix A.

4. Application study: hydrocracking process

To validate the performance of the proposed method, multiple sets of experiments are performed on a practical application, i.e., an industrial hydrocracking process which suffers uncertain disturbances where both modeling and evaluating performance are affected.

4.1. Process description

Hydrocracking process is an important constituent part of the petroleum refining plant. It has a wide range of applications in petrochemical industry due to the efficient green conversion of heavy oil into more economical light oil. Hydrogenation and cracking are the two main reactions in the hydrocracking process. The flowchart of the hydrocracking process is shown in Fig. 5. It is composed of hydrofining (HF), hydrocracking (HC), high and low pressure separation (HPS/LPS) and fractionation parts. Heavy vacuum gas oil (HVGO) is the feed materials and the products are light ends, light naphtha, heavy naphtha, kerosene, diesel and bottom oil. Hydrofining is the first stage of hydrocracking process in which the preheated HVGO and hydrogen enter the stage at the same time. Sulfur and nitrogen compounds are converted to hydrogen sulfide and ammonia, which are subsequently removed in the hydrofining stage. The liquid effluent from the hydrofining is then transmitted to the hydrocracking reactor where most of the cracking reactions take place in liquid phase. The HF and HC consist of three or four beds where recycling H_2 is used to cool the reaction mixtures and control the reaction temperature. The reactor output is combined with water to reduce the corrosion of ammonia on the pipes. Meanwhile, the effluent is supplied to the HPS where it is separated into hydrogen-rich gas, liquid hydrocarbon and water. The hydrogen-rich gas is mixed with hydrogen make-up and recycled back to the reactor section. Then, the hydrocarbon liquid is sent to the LPS where H_2S and NH_3 are recovered. Finally, the liquid hydrocarbon product is fed into the fractionation section where it is separated into different products.

4.2. Experiment setting

To assess the operating performance online, five operating performance levels are determined offline in advance based on product quality, which are optimal, good, general, poor and unqualified. The key product quality indicators shown in Table 1 are selected as the evaluation indicators for the operating performance evaluation

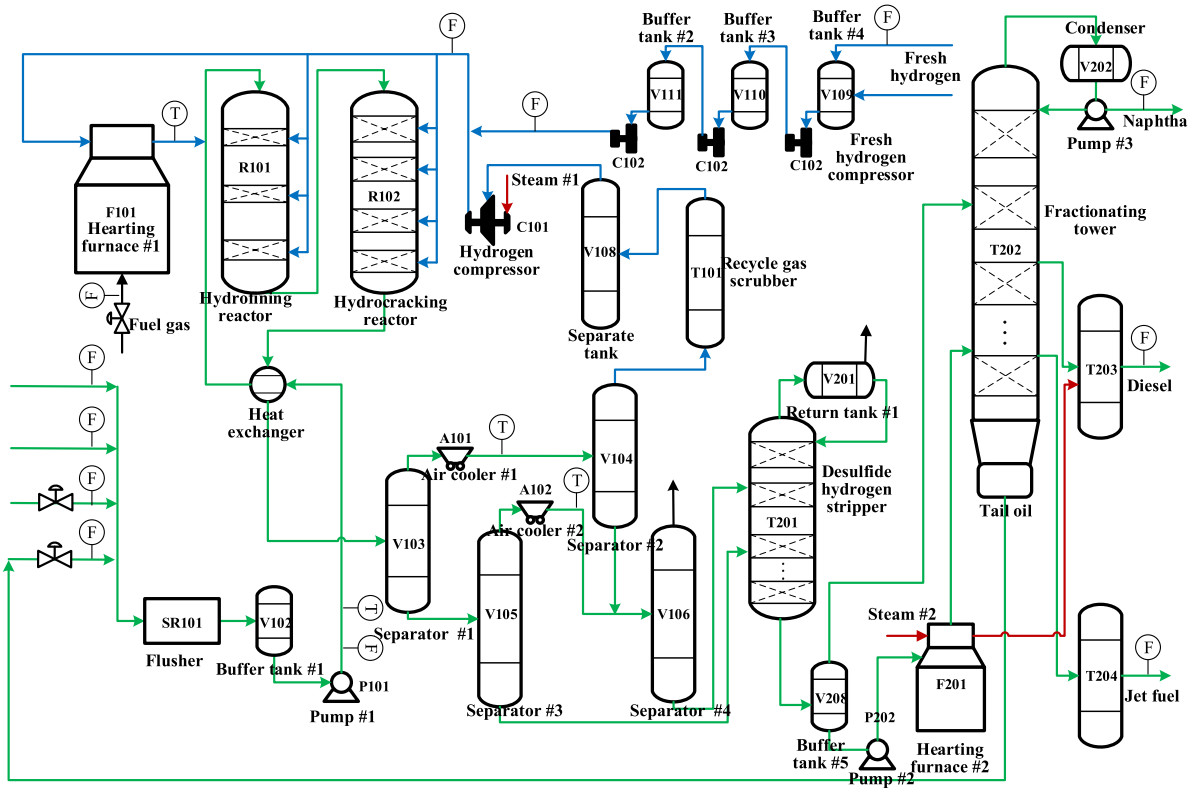

Fig. 5. Flowchart of the hydrocracking process.

Table 1
The key product quality indicators of the hydrocracking process.

No.	Key product quality indicators
1	Content of C4 of light naphtha
2	Content of C5 of light naphtha
3	Final boiling point of heavy naphtha
4	Content of sulfur of heavy naphtha
5	10% distillation temperature of aviation kerosene
6	Final boiling point of aviation kerosene
7	Flash point of aviation kerosene
8	Freezing point of aviation kerosene
9	95% distillation temperature of diesel oil
10	Content of sulfur of diesel oil
11	Density of diesel oil
12	Flash point of diesel oil

of the hydrocracking process through mechanism analysis. The operating performance of the hydrocracking process can be divided into 5 levels based on the historical data of these evaluation indicators. The smaller the evaluation indicator value, the better the operating performance. Among them, "A" represents the level of optimal, "B" represents the level of good, "C" represents the level of normal, "D" represents the level of poor and "E" represents the level of unqualified. The detailed information of evaluation indicators, operating performance levels and operating performance labels can be found in the research proposed by Li et al. (Li et al., 2019).

4.3. Simulation steps

To test the proposed scheme and evaluate the real process, the following simulation steps are taken.

Step 1: Variable selection.

Taking the 10% distillation temperature of aviation kerosene (10%DT-AK) as an example, the effectiveness of the variable selection method is verified by comparing the performance of the prediction models established based on different sets of variables. The modeling performance is evaluated by root-mean-squared errors (RMSE), which can be defined as Eq. (27).

$$RMSE = \sqrt{\frac{1}{L}\sum_{k=1}^{L}(y(k) - \hat{y}(k))^2}, \tag{27}$$

where $y(k)$ denotes the actual value of the evaluation indicator, $\hat{y}(k)$ represents the predictive value.

First, 38 process variables are selected based on mechanism analysis. Then, the sample set of these 38 process variables is collected, including 2016 samples. After that, the discretization degree, partial correlation coefficient and sensitivity index are calculated. The partial results are shown in Table 2.

Based on the process analysis and trial and error, the threshold of the sensitivity index is selected as 0.01. From Table 2, it can be seen that the sensitivity index values of the 12th, 13th, 23th, 31th, 37th, and 38th parameters are lower than other parameters. Therefore, the remaining 32 parameters except the above 6 parameters are determined as sensitive variables.

After that, 320 normal samples are selected to construct the WCMS, and another 120 abnormal samples are selected for validation. The specific distribution of CMDs of the normal samples and abnormal samples are shown in Fig. 6, in which the weight of MDs and CSs are 0.84 and 0.16, respectively. It is found that the CMDs of the normal samples fluctuates around 1, and the average value is 1.0283. However, the CMDs of the abnormalities are much larger than 1, and the average value is 208.5026. Moreover, there are almost no overlap between the CMDs of the normal samples and the abnormal samples, which means the constructed WCMS is effective. In particular, the MD, CS and CMD of the 3th abnormal

Table 2
Sensitivity index of the mechanism selection variables of hydrocracking process.

No.	Parameters	Partial correlation coefficient	Discretization degree	Sensitivity index (SI)
1	Raw oil flow	0.5784	0.1211	0.0700
2	Inlet temperature of heating furnace	0.4035	0.0408	0.0165
...	...	...	...	...
11	Outlet temperature of the third bed of HF	0.4132	0.2690	0.1112
12	Bottom temperature of HF	0.2873	0.0107	0.0031
13	Differential pressure of HF	0.2312	0.0258	0.0060
...	...	...	...	...
21	Cold low oil flow of LPS	0.4756	0.1239	0.0589
22	New hydrogen flow	0.4829	1.5620	0.7543
23	Overhead reflux flow of desulfurization hydrogen stripper	0.0931	0.0834	0.0078
...	...	...	...	...
30	Extraction flow of the middle column of fractionating tower	0.4561	0.0365	0.0166
31	Return temperature of the middle column of fractionating tower	0.2578	0.0171	0.0044
...	...	...	...	...
37	Overhead temperature of diesel stripper	0.3006	0.0311	0.0093
38	Bottom temperature of diesel stripper	0.1722	0.0205	0.0035

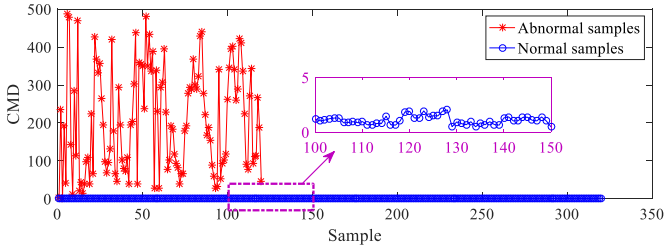

Fig. 6. Specific distribution of CMDs of the normal and abnormal samples.

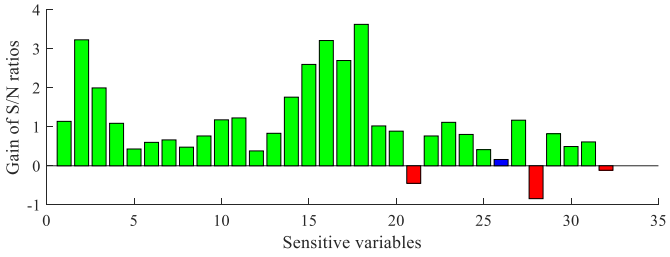

Fig. 7. The histogram of the gain of S/N ratios.

Table 3
OAs and S/N ratios.

Variables	1	2	...	15	16	SN1	SN2	ΔSN
$x_1(x_1)$	1	1	...	2	2	1.269	0.131	1.14
$x_2(x_2)$	1	1	...	1	1	1.058	−2.169	3.23
...	...	...	...	...	...	...	...	...
$x_{20}(x_{23})$	2	1	...	2	1	0.886	0.122	0.76
$x_{21}(x_{25})$	2	1	...	1	1	−0.296	0.154	−0.45
...	...	...	...	...	...	...	...	...
$x_{26}(x_{31})$	2	1		2	2	1.230	1.069	0.16
$x_{27}(x_{32})$	2	2		1	2	2.650	1.482	1.17
$x_{28}(x_{33})$	2	2	...	1	2	−0.356	0.487	−0.84
...	...	...	...	...	...	...	...	...
$x_{31}(x_{36})$	2	2	...	1	1	1.632	1.021	0.61
$x_{32}(x_{37})$	2	2	...	1	2	−0.610	−0.495	−0.12

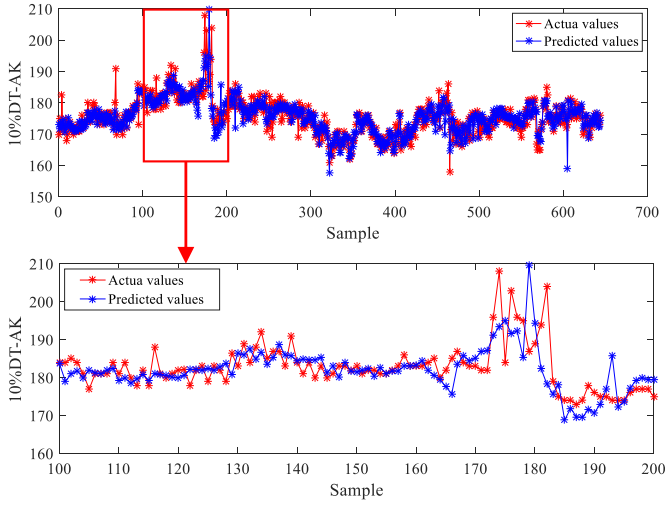

Fig. 8. Prediction performance for the 10% distillation temperature of aviation kerosene based on key sensitive variable set.

Table 4
The RMSE of JITL-PPCR on three variable sets.

Variable set	RMSE
Mechanism selection variable set	3.5754
Sensitive variable set	3.4107
Key sensitive variable set	3.2699

sample are 1.657, 5.3472 and 2.2475, respectively. If only the MD is used to identify the sample, it appears to be a normal sample. However, according to the CS and CMD, the sample should be abnormal, which is the same as the actual situation. Thus, compared with the MTS, WCMTS performs much better.

To optimize WCMS, an OAs is designed in Table 3 where the variables in the parentheses correspond to the process variables originally selected. The histogram of the gain of S/N ratios is shown in Fig. 7.

As shown in Table 3 and Fig. 7, the ΔSN of the 21th, 28th, 32th sensitive variables are negative, which means these variables are useless for model training. Moreover, the 26th sensitive variable has a smallΔSN, which indicates that this variable has little effect on modeling. Therefore, 28 key sensitive variables are finally selected for modeling.

To verify the effectiveness of the variable selection method, another 1610 samples of 10%DT-AK from March 21, 2016 to November 30, 2018 are collected, which contains multiple working conditions. There are 966 samples for training the JITL-PPCR model, and 644 samples for testing. The variables are divided into mechanism selection variables, sensitive variables, and key sensitive variables, respectively. Figs. 8–10 show the comparisons of the actual and predicted values, where the red and blue lines represent the actual and predicted output trends, respectively. Table 4 shows the RMSE of JITL-PPCR based on three variable sets. Compared with other two variable sets, the prediction results based on key sen-

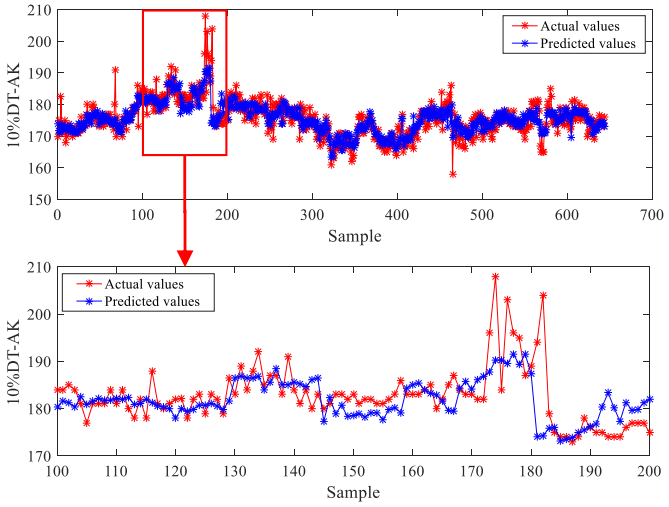

Fig. 9. Prediction performance for the 10% distillation temperature of aviation kerosene based on sensitive variable set.

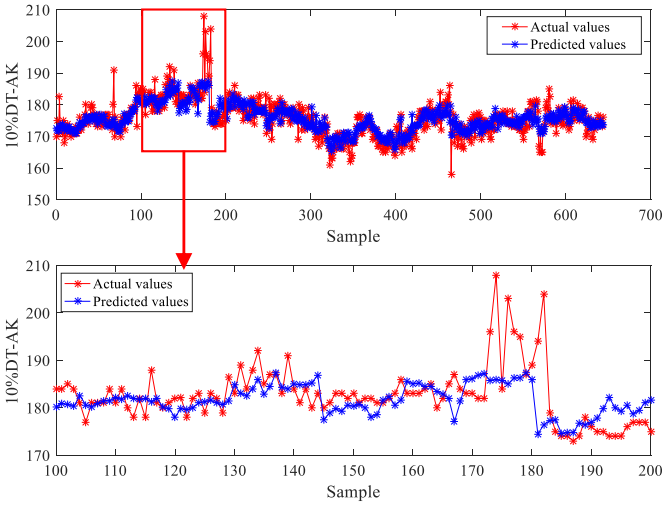

Fig. 10. Prediction performance for the 10% distillation temperature of aviation kerosene based on original process variable set.

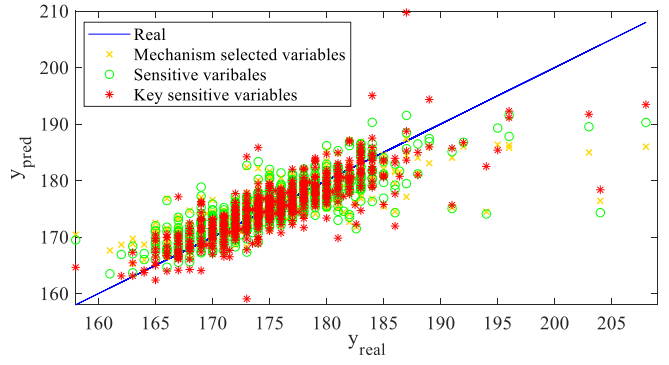

Fig. 11. Scatter plot of the real and predicted outputs on the three variable sets.

sitive variables can better track the actual value. Furthermore, the scatter plots of the predicted and actual outputs are also compared for method with different variable sets, which is shown in Fig. 11. In the figure, if the predictions are exactly accurate, the points should lie on the diagonal line. From Fig. 11, it can be seen that the model based on key sensitive variables has the most points that are close to the diagonal line. It means the variable selection

Table 5
The RMSE of four methods based on three auxiliary variable sets.

Variable set	RMSE			
	PLS	SVM	LWKPCR	LWPLS
Mechanism selection variable set	3.6553	3.9652	3.2358	3.2870
Sensitive variabel set	3.5363	3.8422	3.1727	3.1740
Key sensitive variable set	3.4955	3.7272	3.0377	3.0474

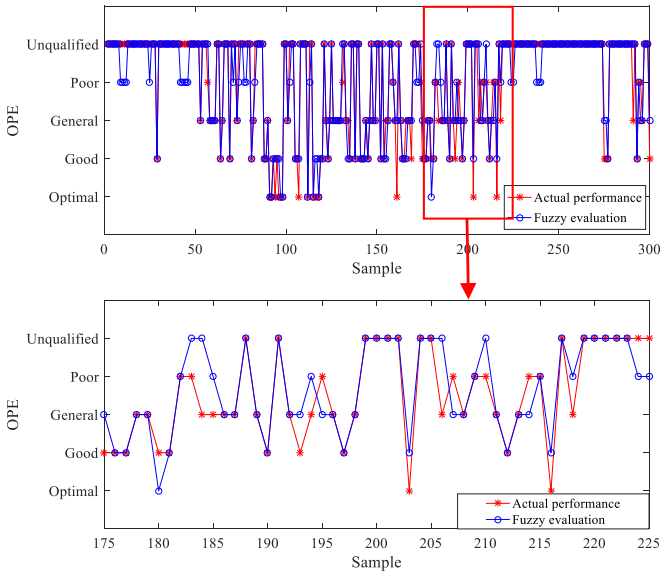

Fig. 12. Comparison of actual operating performance and fuzzy synthetic evaluation results.

method is effective. Note that the prediction accuracy of the samples with relatively high values is not very high due to the completeness of the modeling data set. However, although the prediction accuracy of the above samples is not very high, the accuracy is still within the input accuracy range allowed by the PFES, which has little impact on the evaluation. In fact, the proposed probabilistic fuzzy evaluation strategy also considers the existence of certain errors in the prediction results of evaluation indicators.

In addition, partial least squares (PLS), support vector machine (SVM), local weighted kernel principal component regression (LWKPCR) (Yuan et al., 2014), and locally weighted partial least squares (LWPLS) (Yuan et al., 2016) are further used to verify the effectiveness of the proposed method. Table 5 shows the RMSE of these four methods based on three different variable sets. From Table 4, the prediction results based on key sensitive variables have the highest accuracy among all variable sets, which indicates that the proposed method is effective for variable selection.

Step 2: Online operating performance evaluation.

The KSV obtained from *Step* 1 will be used for estimation of the evaluation indicators shown in Table 1.

Experiment I: This experiment is carried out to validate the effectiveness and applicability of the probabilistic fuzzy evaluation method. The evaluation performance will be compared in terms of accuracy defined as Eq. (28).

$$accuracy = \frac{\text{The number of evaluation results consistent with the labels}}{\text{Total number of labels}} \times 100\%. \quad (28)$$

Comparative results of probabilistic fuzzy evaluation, fuzzy synthetic evaluation and the method proposed by Li et al. (Li et al., 2019) are shown in Figs. 12–14 and Table 6, which can be summarized as follows.

Table 6
The accuracy of fuzzy synthetic evaluation, the method proposed by Li et al. and probabilistic fuzzy evaluation.

Methods	Operating performance grade						Accuracy
	A	B	C	D	E	sum	
Offline label	15	38	48	12	186	299	–
Fuzzy evaluation	7	31	39	5	161	243	0.813
The method proposed by Li et al.	10	32	39	6	173	260	0.870
Probabilistic fuzzy evaluation	11	35	44	7	177	274	0.916

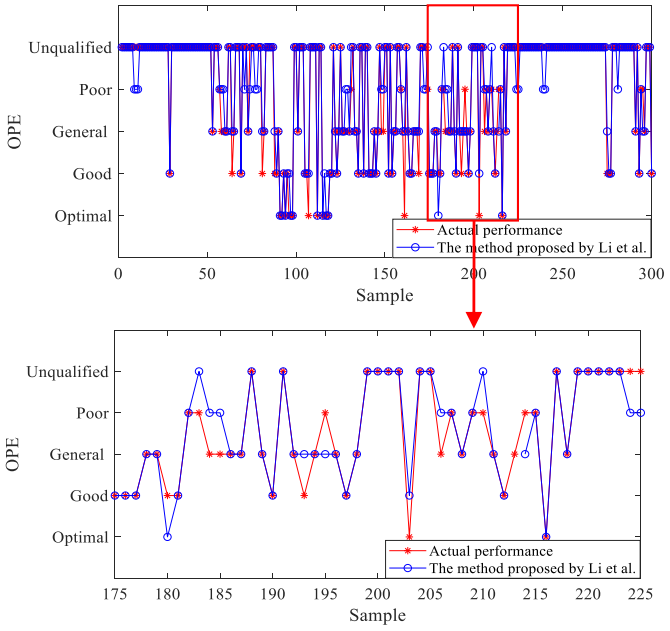

Fig. 13. Comparison of actual operating performance and the evaluation results based on the method proposed by Li et al.

(1) Compared with traditional fuzzy synthetic evaluation and the method proposed by Li et al., the process operating performance can be more accurately assessed by applying probabilistic fuzzy evaluation, which can achieve accurately online OPE for complex industrial processes. The performance of the method proposed by Li et al. is better than the traditional fuzzy synthetic evaluation due to its two-layer fuzzy synthetic strategy.
(2) Moreover, it is obvious that the use of probabilistic fuzzy evaluation for each operating performance level can get better evaluation accuracy, with an overall accuracy improvement of 10.3% and 4.6% compared with the traditional fuzzy synthetic evaluation and the method proposed by Li et al., respectively. Therefore, probabilistic fuzzy evaluation is superior to traditional fuzzy synthetic evaluation and the method proposed by Li et al..

Experiment II: This experiment is carried out to test the performance of the proposed probabilistic fuzzy evaluation method under the more complex environment where an extra stochastic variation ζ_n is added in the original evaluation indicator data $y(k)$. The stochastic variation ζ_n can be defined as

$$\zeta_n \sim N(0, \sigma_n^2), \tag{29}$$

where suppose ζ_n follows a Gaussian distribution, σ_n is the standard deviation of the random noise that will gradually change in the following pattern to simulate the complex and poor environment.

$$\sigma_n = \{0.5\%\sigma_y, 1\%\sigma_y, 1.5\%\sigma_y, \cdots, 4.5\%\sigma_y, 5\%\sigma_y\}, \tag{30}$$

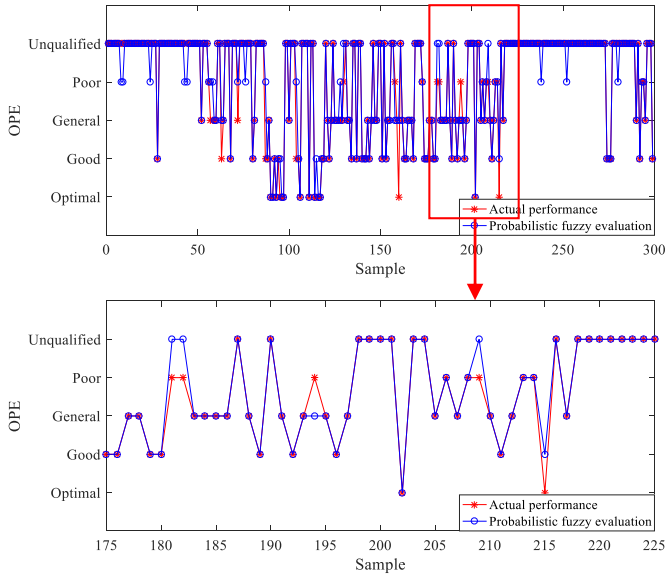

Fig. 14. Comparison of actual operating performance and probabilistic fuzzy evaluation results.

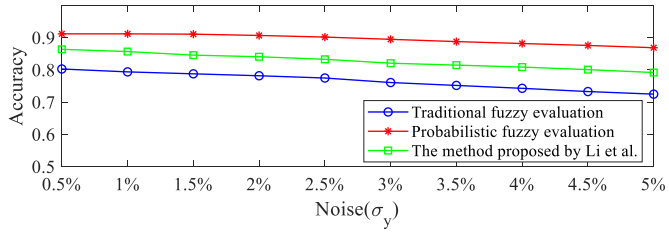

Fig. 15. The accuracy of the probabilistic fuzzy evaluation, the method proposed by Li et al. and traditional fuzzy synthetic evaluation with different standard deviation of noise.

where σ_y represents the standard deviation of the predictive evaluation indicator. The accuracy of the probabilistic fuzzy evaluation, the method proposed by Li et al. and the traditional fuzzy synthetic evaluation is shown in Fig. 15. It can be seen that as the standard deviation of the added noise increases from $0.5\%\sigma_y$ to $5\%\sigma_y$, compared with the traditional fuzzy synthetic evaluation and the method proposed by Li et al., the probabilistic fuzzy evaluation can still achieve better accuracy.

5. Conclusion

In this paper, an online evaluation approach using probabilistic fuzzy is proposed to improve the evaluation performance for chemical processes with uncertainties. In the modeling step, the probability distributions of evaluation indicators are estimated via JITL-PPCR, which is of great benefit because of considering process uncertainties in establishing evaluation indicator phase. For variable selection, the WCMTS method, which can find more effec-

tive KSV than original variables, is then developed for improving prediction accuracy. By the use of probabilistic interpretation, the fuzzy synthetic evaluation is successfully extended to probabilistic frameworks in the evaluation step. Sufficient experiment results show that, the proposed probabilistic fuzzy evaluation method can achieve better accuracy than these previous methods.

Declaration of Competing Interest

None

CRediT authorship contribution statement

Yalin Wang: Supervision, Project administration, Funding acquisition. **Ling Li:** Conceptualization, Methodology, Software, Data curation, Writing - original draft. **Kai Wang:** Writing - review & editing.

Acknowledgment

This work was supported in part by National Natural Science Foundation of China (NSFC) (61590921, U1911401), in part by National Key Research and Development Program of China (2018AAA0101603), in part by the Foundation for Innovative Research Groups of the National Natural Science Foundation of China (61621062), in part by the Natural Science Foundation of Hunan Province of China (2018JJ3687), and in part by Innovation-driven plan in Central South University (2018CX011) .

Appendix A

Derivation of probabilistic fuzzy membership functions

For probabilistic fuzzy membership functions, suppose the evaluation indicator $x \sim N(\hat{x}, \sigma_x)$ as follows:

$$p(x) = \exp\left(-\frac{(x-\hat{x})^2}{2\sigma_x^2}\right). \tag{A1}$$

Then, the S-shaped probabilistic fuzzy membership functions can be derived as follows:

$$\begin{aligned}
\varphi^j(x)' &= \int_{-\infty}^{\alpha^j} \exp\left(-\frac{(x-\hat{x})^2}{2\sigma_x^2}\right)dx \\
&+ \int_{\alpha^j}^{\frac{\alpha^j+\beta^j}{2}} \left(1-2\left(\frac{x-\alpha^j}{\beta^j-\alpha^j}\right)^2\right)\exp\left(-\frac{(x-\hat{x})^2}{2\sigma_x^2}\right)dx \\
&+ \int_{\frac{\alpha^j+\beta^j}{2}}^{\beta^j} 2\left(\frac{x-\beta^j}{\beta^j-\alpha^j}\right)\exp\left(-\frac{(x-\hat{x})^2}{2\sigma_x^2}\right)dx \\
&= \int_{-\infty}^{0} \exp\left(-\frac{(x-\hat{x})^2}{2\sigma_x^2}\right)dx + \int_{0}^{\alpha^j} \exp\left(-\frac{(x-\hat{x})^2}{2\sigma_x^2}\right)dx. \\
&+ \int_{\alpha^j}^{\frac{\alpha^j+\beta^j}{2}} \exp\left(-\frac{(x-\hat{x})^2}{2\sigma_x^2}\right)dx \\
&+2\int_{\alpha^j}^{\frac{\alpha^j+\beta^j}{2}} \left(\frac{x-\alpha^j}{\beta^j-\alpha^j}\right)^2\exp\left(-\frac{(x-\hat{x})^2}{2\sigma_x^2}\right)dx \\
&+ \int_{\frac{\alpha^j+\beta^j}{2}}^{\beta^j} 2\left(\frac{x-\beta^j}{\beta^j-\alpha^j}\right)\exp\left(-\frac{(x-\hat{x})^2}{2\sigma_x^2}\right)dx
\end{aligned} \tag{A2}$$

For simplicity, suppose that $u = \frac{x-\hat{x}}{\sqrt{2}\sigma_x}, k_1 = \frac{\alpha^j-\hat{x}}{\sqrt{2}\sigma_x}, k_2 = \frac{(\alpha^j+\beta^j)/2-\hat{x}}{\sqrt{2}\sigma_x}, k_3 = \frac{\beta^j-\hat{x}}{\sqrt{2}\sigma_x}$.

Therefore

$$\begin{aligned}
\varphi^j(u)' &= \int_{-\infty}^{-\frac{\hat{x}}{\sqrt{2}\sigma_x}} \sqrt{2}\sigma_x \exp\left(-u^2\right)du \\
&+ \int_{-\frac{\hat{x}}{\sqrt{2}\sigma_x}}^{k_1} \sqrt{2}\sigma_x \exp\left(-u^2\right)du + \int_{k_1}^{k_2} \sqrt{2}\sigma_x \exp\left(-u^2\right)du \\
&+ \frac{4\sqrt{2}\sigma_x^3}{\left(\beta^j-\alpha^j\right)^2}\int_{k_1}^{k_2}\left(u^2+2\left(\frac{\hat{x}-\alpha^j}{\sqrt{2}\sigma_x}\right)u+\left(\frac{\hat{x}-\alpha^j}{\sqrt{2}\sigma_x}\right)^2\right), \\
&\exp\left(-u^2\right)du \\
&+ \frac{4\sqrt{2}\sigma_x^3}{\left(\beta^j-\alpha^j\right)^2}\int_{k_2}^{k_3}\left(u^2+2\left(\frac{\hat{x}-\beta^j}{\sqrt{2}\sigma_x}\right)u+\left(\frac{\hat{x}-\beta^j}{\sqrt{2}\sigma_x}\right)^2\right) \\
&\exp\left(-u^2\right)du
\end{aligned} \tag{A3}$$

$$\begin{aligned}
\varphi^j(x)' &= \sqrt{\frac{\pi}{2}}\sigma_x + \frac{2\sqrt{2}\sigma_x^3}{\left(\beta^j-\alpha^j\right)}k_3\exp(-k_1^2) \\
&-\left(\frac{4\sqrt{2}\sigma_x^3}{\left(\beta^j-\alpha^j\right)^2}k_1 + \frac{4\sqrt{2}\sigma_x^3}{\left(\beta^j-\alpha^j\right)^2}k_3\right)\exp\left(-k_2^2\right) \\
&+\frac{6\sqrt{2}\sigma_x^3}{\left(\beta^j-\alpha^j\right)^2}k_3\exp\left(-k_3^2\right) + \frac{2\sqrt{2}\sigma_x^3\left(1+2k_1^2\right)}{\left(\beta^j-\alpha^j\right)^2}erf(k_1) \\
&+\left(\sqrt{2}\sigma_x - \frac{4\sqrt{2}\sigma_x^3}{\left(\beta^j-\alpha^j\right)^2} - \frac{4\sqrt{2}\sigma_x^3}{\left(\beta^j-\alpha^j\right)^2}k_1^2 - \frac{4\sqrt{2}\sigma_x^3}{\left(\beta^j-\alpha^j\right)^2}k_3^2\right)erf(k_2) \\
&+\frac{6\sqrt{2}\sigma_x^3}{\left(\beta^j-\alpha^j\right)^2}erf(k_3)
\end{aligned} \tag{A4}$$

Thus, the S-shaped probabilistic fuzzy membership can be summarized as (A4).

Similarity, for simplicity, suppose that $u = \frac{x-\hat{x}}{\sqrt{2}\sigma_x}, t_1 = \frac{c^j-\hat{x}}{\sqrt{2}\sigma_x}, t_2 = \frac{(c^j+d^j)/2-\hat{x}}{\sqrt{2}\sigma_x}, t_3 = \frac{d^j-\hat{x}}{\sqrt{2}\sigma_x}$, then the Z-shaped probabilistic fuzzy membership functions can be derived as follows:

$$\begin{aligned}
\psi^j(u)' &= \frac{4\sqrt{2}\sigma_x^3}{\left(d^j-c^j\right)^2}\left(\int_{t_1}^{t_2} u^2\exp\left(-u^2\right)du + \int_{t_1}^{t_2} -2t_1 u\exp\left(-u^2\right)du\right. \\
&\left.+\int_{t_1}^{t_2} t_1^2\exp\left(-u^2\right)du\right) \\
&+\int_{t_2}^{t_3}\sqrt{2}\sigma_x\exp\left(-u^2\right)du + \int_{t_3}^{+\infty}\sqrt{2}\sigma_x\exp\left(-u^2\right)du \\
&+\frac{4\sqrt{2}\sigma_x^3}{\left(d^j-c^j\right)^2}\left(\int_{t_2}^{t_3} u^2\exp\left(-u^2\right)du + \int_{t_2}^{t_3} -2t_3 u\exp\left(-u^2\right)du\right. \\
&\left.+\int_{t_2}^{t_3} t_3^2\exp\left(-u^2\right)du\right)
\end{aligned} \tag{A5}$$

$$\psi^j(x)' = \sqrt{\frac{\pi}{2}}\sigma_x - \frac{2\sqrt{2}\sigma_x^3}{\left(d^j - c^j\right)^2} t_1 \exp\left(-t_1^2\right)$$
$$+\left(\frac{4\sqrt{2}\sigma_x^3}{\left(d^j - c^j\right)^2}(t_1 - t_2)\right)\exp\left(-t_2^2\right)$$
$$+\frac{2\sqrt{2}\sigma_x^3}{\left(d^j - c^j\right)^2} t_3 \exp\left(-t_3^2\right) + \frac{4\sqrt{2}\sigma_x^3}{\left(d^j - c^j\right)^2}\left(\frac{1}{2} - t_1^2\right) erf(t_1). \quad \text{(A6)}$$
$$+\left(\frac{4\sqrt{2}\sigma_x^3}{\left(d^j - c^j\right)^2}\left(t_1^2 - t_3^2\right) - \sqrt{2}\sigma_x\right) erf(t_2)$$
$$-\left(\frac{2\sqrt{2}\sigma_x^3}{\left(d^j - c^j\right)^2}\left(1 - 2t_3^2\right)\right) erf(t_3)$$

Thus, the Z-shaped probabilistic fuzzy membership can be summarized as (A6).

For the Gaussian-shaped membership functions, the derivation process can be presented as follows:

$$\mu_i^j(x)' = \int_{-\infty}^{+\infty} \exp\left(-\frac{\left(x - \xi_i^j\right)^2}{2\left(\sigma_i^j\right)^2}\right) \bullet \exp\left(-\frac{(x - \widehat{x})^2}{2\sigma_x^2}\right) dx$$
$$= \int_{-\infty}^{+\infty} \exp\left(-\frac{\left(x - \xi_i^j\right)^2}{2\left(\sigma_i^j\right)^2} - \frac{(x - \widehat{x})^2}{2\sigma_x^2}\right) dx$$
$$= \int_{-\infty}^{+\infty} \exp - \left(\left(\sigma_x^2 + \left(\sigma_i^j\right)^2\right)\left(x - \frac{\sigma_x^2\xi_i^j + \left(\sigma_i^j\right)^2\widehat{x}}{\sigma_x^2 + \left(\sigma_i^j\right)^2}\right)^2\right.$$
$$\left. + \left(\sigma_x^2\left(\xi_i^j\right)^2 + \left(\sigma_i^j\right)^2\widehat{x}^2\right) - \frac{\left(\sigma_x^2\xi_i^j + \left(\sigma_i^j\right)^2\widehat{x}\right)^2}{\sigma_x^2 + \left(\sigma_i^j\right)^2}\right) dx$$
$$= \exp\left(-\left(\sigma_x^2\left(\xi_i^j\right)^2 + \left(\sigma_i^j\right)^2\widehat{x}^2 - \frac{\left(\sigma_x^2\xi_i^j + \left(\sigma_i^j\right)^2\widehat{x}\right)^2}{\sigma_x^2 + \left(\sigma_i^j\right)^2}\right)\right) \cdot \quad \text{(A7)}$$
$$\bullet \int_{-\infty}^{+\infty} \exp - \left(\left(\sigma_x^2 + \left(\sigma_i^j\right)^2\right)\left(x - \frac{\sigma_x^2\xi_i^j + \left(\sigma_i^j\right)^2\widehat{x}}{\sigma_x^2 + \left(\sigma_i^j\right)^2}\right)^2\right) dx$$
$$= \sqrt{\frac{\pi}{\left(\sigma_x^2 + \left(\sigma_i^j\right)^2\right)^3}}\left(\left(\sigma_x^2\xi_i^j + \left(\sigma_i^j\right)^2\widehat{x}\right)^2\right)$$
$$\exp\left(-\left(\sigma_x^2\left(\xi_i^j\right)^2 + \left(\sigma_i^j\right)^2\widehat{x}^2 - \frac{\left(\sigma_x^2\xi_i^j + \left(\sigma_i^j\right)^2\widehat{x}\right)^2}{\sigma_x^2 + \left(\sigma_i^j\right)^2}\right)\right)$$

References

Chang, Y., Zou, X., Wang, F., Zhao, L., Zheng, W., 2018. Multi-mode plant-wide process operating performance assessment based on a novel two-level multi-block hybrid model. Chem. Eng. Res. Des. 136, 721–733.

Chang, Z., Li, Y., Fatima, N., 2019. A theoretical survey on Mahalanobis-Taguchi system. Measurement 136, 501–510.

Chen, H., Jiang, B., 2019. A review of fault detection and diagnosis for the traction system in high-speed trains. IEEE Trans. Intell. Transp. doi:10.1109/TITS.2019.2897583.

Chen, H., Jiang, B., Ding, S., Lu, N., Chen, W., 2019a. Probability-relevant incipient fault detection and diagnosis methodology with applications to electric drive systems. IEEE Trans. Control Syst. Technol. 27, 2766–2773.

Chen, J., Yang, C., Zhou, C., Li, Y., Zhu, H., Gui, W., 2019b. Multivariate regression model for industrial process measurement based on double locally weighted partial lease squares. IEEE Trans. Instrum. Meas. doi:10.1109/TIM.2019.2943824.

Chen, K., Huang, M., Chang, P., 2006. Performance evaluation on manufacturing times. Int. J. Adv. Manuf. Tech. 31, 335–341.

Fuat, D., Ahmet, P., Jose, A., 2003. R. Orthogonal nonlinear partial least-squares regression. Ind. Eng. Chem. Res. 42, 5836–5849.

Ge, Z., Song, Z., 2010. A comparative study of just-in-time-learning based methods for online soft sensor modeling. Chemometr. Intell. Lab. Syst. 104, 306–317.

Hiromasa, K., Kimito, F., 2013. Adaptive soft sensor model using online support vector regression with time variable and discussion of appropriate hyperparamter settings and window size. Comput. Chem. Eng. 58 (11), 288–297.

Jiang, F., Sui, Y., Zhou, L., 2015. A relative decision entropy-based feature selection approach. Pattern Recogn. 48, 2151–2163.

Kumar, B.S., Sudhakar, K., 2015. Performance evaluation of 10MW grid connected solar photovoltaic power plant in India. Energy Rep. 1, 184–192.

Kumar, M., Weippert, M., Vilbrandt, R., Kreuzfeld, S., Stoll, R., 2007. Fuzzy evaluation of heart rate signals for mental stress assessment. IEEE Trans. Fuzzy Syst. 15, 791–808.

Li, L., Yuan, X., Wang, Y., Sun, B., Wu, D., 2019. A two-layer fuzzy synthetic strategy for operational performance assessment of an industrial hydrocracking process. Control Eng. Pract. doi:10.1016/j.conengprac.2019.104187.

Liu, J., Li, R., Wu, R., 2014a. Feature selection for varying coefficient models with ultrahigh dimensional covariates. J. Am. Stat. Assoc. 109, 266–274.

Liu, Y., Chang, Y., Wang, F., 2014b. Online process operating performance assessment and nonoptimal cause identification for industrial processes. J. Process Control 24, 1548–1555.

Liu, Y., Wang, F., Chang, Y., 2016. Operating optimality assessment and nonoptimal cause identification for multimode industrial process with transitions. Can. J. Chem. Eng. 94, 1342–1353.

Liu, Y., Wang, X., Wang, F., Gao, F., 2018. Gaussian process regression and bayesian inference based operating performance assessment for multiphase batch processes. Ind. Eng. Chem. Res. 57, 7232–7244.

Mahalakshmi, P., Ganesan, K., 2009. Mahalanobis Taguchi system based criteria selection for shrimp aquaculture development. Comput. Electron. Agric. 65, 192–197.

Molinos-Senante, M., Gómez, T., Garrido-Baserba, M., Caballero, R., Sala-Garrido, R., 2014. Assessing the sustainability of small wastewater treatment systems: a composite indicator approach. Sci. Total Environ. 497-498, 607–617.

Nishiguchi, J., Takai, T., 2010. IPL2 and 3 performance improvement method for process safety using event correlation analysis. Comput. Chem. Eng. 34 (12), 2007–2013.

Pai, T.Y., Wan, T.J., Hsu, S.T., Chang, C.T., Tsai, Y.P., Lin, C.Y., Su, H.C., Yu, L.F., 2009. Using fuzzy inference system to improve neural network for predicting hospital wastewater treatment plant efflent. Comput. Chem. Eng. 33 (7), 1272–1278.

Qi, C., Li, H., Zhang, X., Zhao, X., Li, S., Gao, F., 2011. Time/space-separation-based svm modeling for nonlinear distributed parameter processes. Ind. Eng. Chem. Res. 50, 332–341.

Sedghi, S., Sadeghian, A., Huang, B., 2017. Mixture semisupervised probabilistic principal component regression model with missing inputs. Comput. Chem. Eng. 103, 176–187.

Soylemezoglu, A., Jagannathan, S., Saygin, C., 2011. Mahalanobis-Taguchi system as a multi-sensor based decision making prognostics tool for centrifugal pump failures. IEEE Trans. Reliab. 60, 864–878.

Sun, B., Yang, C., Wang, Y., Gui, W., Craig, I., Olivier, L., 2020. A comprehensive hybrid first principles/machine learning modeling framework for complex industrial process. J. Process Control 86, 30–43.

Sun, X., Liu, Y., Xu, M., Chen, H., Han, J., Wang, K., 2013. Feature selection using dynamic weights for classification. Knowl.-Based Syst. 37, 541–549.

Takagi, T., Sugeno, M., 1993. Fuzzy identification of systems and its applications to modeling and control. Read. Fuzzy Sets Intell. Syst. 15, 387–403.

Wang, K., Chen, J., Song, Z., 2019a. Using multivariate pattern segmentation to assess process performance and mine good operation conditions for dynamic chemical industry. Chem. Eng. Sci. 201, 339–348.

Wang, K., Chen, J., Song, Z., 2020. A sparse loading-based contribution method for multivariate control performance diagnosis. J. Process Control 85, 199–213.

Wang, Y., Pan, Z., Yuan, X., Yang, C., Gui, W., 2019b. A novel deep learning based fault diagnosis approach for chemical process with extended deep belief network. ISA Trans. doi:10.1016/j.isatra.2019.07.001.

Wu, J., Xie, Y., Yang, C., Gui, W., 2014. An unsupervised reduction method for the selection of flotation froth image characters and its application. Inf. Control 43, 314–317.

Yang, A., Martin, E., Morris, J., 2011. Identification of semi-parametrtic hybrid process models. Comput. Chem. Eng. 35 (1), 63–70.

Yuan, X., Ge, Z., Song, Z., 2014. Locally weighted kernel principal component regression model for soft sensing of nonlinear time-variant process. Ind. Eng. Chem. Res. 53, 13736–13749.

Yuan, X., Ge, Z., Song, Z., 2016. Spatio-temporal adaptive soft sensor for nonlinear time-varying and variable drifting processes based on moving window LWPLS and time difference model. Asia-Pac. J. Chem. Eng. 11, 209–219.

Yuan, X., Zhou, J., Wang, Y., Yang, C., 2018. Multi-similarity measurement driven ensemble just-in-time learning for soft sensing of industrial processes. J. Chemometr. doi:10.1002/cem.3040.

Zhang, B., Yang, C., Zhu, H., Li, Y., Gui, W., 2016. Evaluation strategy for the control of the copper removal process based on oxidation-reduction potential. Chem. Eng. J. 284, 294–304.

Zheng, J., Song, Z., 2017. Linear subspace principal component regression model for quality estimation of nonlinear and multimode industrial processes. Ind. Eng. Chem. Res. 56, 6275–6285.
Zhou, L., Jia, L., Wang, Y., 2020. A just-in-time-learning based two-dimensional control strategy for nonlinear batch processes. Inf. Sci. 507, 220–239.
Zhu, J., Ge, Z., Song, Z., 2015. Robust semi-supervised mixture probabilistic principal component regression model development and application to soft sensors. J. Process Control 32, 25–37.
Zou, X., Wang, F., Chang, Y., Zhao, L., Zheng, W., 2018. Two-level multi-block operating performance optimality assessment for plant-wide processes. Can. J. Chem. Eng. 96, 2395–2407.